Weak-coupling analysis of the neutron-scattering spectral weight

N. Bulut and D. J. Scalapino
Department of Physics, University of California, Santa Barbara, California 93106-9530
(Received 19 May 1992)

A random-phase approximation for $\chi(\mathbf{q},\omega)$ with a BCS irreducible susceptibility, provides a simple framework for examining the interplay of antiferromagnetic and superconducting correlations. Here we study the neutron-scattering spectral weight in the normal and superconducting states for both an s and a $d_{x^2-y^2}$ gap.

Inelastic neutron-scattering experiments give information on the momentum, energy, and temperature dependence of the spin-fluctuation spectral weight $\mathrm{Im}\chi(\mathbf{q},\omega)$. Recent measurements on the superconducting cuprates provide insight into these spin fluctuations in both the normal and the superconducting phases of these materials.[1-6] In particular, in the superconducting phase these experiments determine the effect of the superconducting pairing correlations on the spin-fluctuation spectrum. Here, using an RPA-like approximation for $\chi(\mathbf{q},\omega)$ in which the irreducible susceptibility is calculated within a BCS framework for both an s- and a $d_{x^2-y^2}$-wave gap, we examine the spectral weight $\mathrm{Im}\chi(\mathbf{q},\omega)$. We have previously used this same approach to analyze NMR Knight shifts and T_1^{-1} measurements as well as T_2^{-1} data.[7-9] Although it is clearly approximate, by treating the Coulomb interaction strength which enters it as an effective parameter, we have found that it provides an excellent fit to the momentum, frequency, and temperature dependence determined from Monte Carlo calculations of the Hubbard model.[10-12] It is also one of the simplest forms which takes into account both antiferromagnetic and pairing correlations. We will see that the resultant spectral weight reflects the features of the underlying gap structure.[13,14,15]

For the single-band Hubbard model, the RPA form for the spin susceptibility is

$$\chi(\mathbf{q},\omega)=\frac{\chi_0(\mathbf{q},\omega)}{1-U\chi_0(\mathbf{q},\omega)} . \tag{1}$$

Here U is a renormalized, reduced Coulomb repulsion, which approximates the effect of multiple particle-particle scattering. In the normal state, $\chi_0(\mathbf{q},\omega)$ is given by the Lindhard function

$$\chi_0(\mathbf{q},\omega)=\frac{1}{N}\sum_{\mathbf{p}}\frac{f(\varepsilon_{\mathbf{p}+\mathbf{q}})-f(\varepsilon_{\mathbf{p}})}{\omega-(\varepsilon_{\mathbf{p}+\mathbf{q}}-\varepsilon_{\mathbf{p}})+i0^+} . \tag{2}$$

Here $\varepsilon_{\mathbf{p}}=-2t[\cos(p_x)+\cos(p_y)]-\mu$ and $f(\varepsilon_{\mathbf{p}})=[\exp(\varepsilon_{\mathbf{p}}/T)+1]^{-1}$ is the usual Fermi factor, with μ the chemical potential and T the temperature. We assume that the renormalized Coulomb potential has no momentum and energy dependence and set its value to $U=2t$. We also choose $\langle n\rangle=0.85$.[16] For fillings near $\langle n\rangle\sim 0.85$, the momentum, energy, and temperature dependence of the magnetic susceptibility calculated using Eqs. (1) and (2) with $U=2t$ is in close agreement with Monte Carlo results obtained using $U=4t$ down to temperatures of order $T=0.2t$.[10-12]

In the superconducting state $\chi_0(\mathbf{q},\omega)$ is replaced by the BCS expression

$$\begin{aligned}\chi_0^{\mathrm{BCS}}(\mathbf{q},\omega)=\frac{1}{N}\sum_{\mathbf{p}}\Bigg[&\frac{1}{2}\left[1+\frac{\varepsilon_{\mathbf{p}+\mathbf{q}}\varepsilon_{\mathbf{p}}+\Delta_{\mathbf{p}+\mathbf{q}}\Delta_{\mathbf{p}}}{E_{\mathbf{p}+\mathbf{q}}E_{\mathbf{p}}}\right]\frac{f(E_{\mathbf{p}+\mathbf{q}})-f(E_{\mathbf{p}})}{\omega-(E_{\mathbf{p}+\mathbf{q}}-E_{\mathbf{p}})+i0^+}\\&+\frac{1}{4}\left[1-\frac{\varepsilon_{\mathbf{p}+\mathbf{q}}\varepsilon_{\mathbf{p}}+\Delta_{\mathbf{p}+\mathbf{q}}\Delta_{\mathbf{p}}}{E_{\mathbf{p}+\mathbf{q}}E_{\mathbf{p}}}\right]\frac{1-f(E_{\mathbf{p}+\mathbf{q}})-f(E_{\mathbf{p}})}{\omega+(E_{\mathbf{p}+\mathbf{q}}+E_{\mathbf{p}})+i0^+}\\&+\frac{1}{4}\left[1-\frac{\varepsilon_{\mathbf{p}+\mathbf{q}}\varepsilon_{\mathbf{p}}+\Delta_{\mathbf{p}+\mathbf{q}}\Delta_{\mathbf{p}}}{E_{\mathbf{p}+\mathbf{q}}E_{\mathbf{p}}}\right]\frac{f(E_{\mathbf{p}+\mathbf{q}})+f(E_{\mathbf{p}})-1}{\omega-(E_{\mathbf{p}+\mathbf{q}}+E_{\mathbf{p}})+i0^+}\Bigg] .\end{aligned} \tag{3}$$

This expression contains the usual coherence factors, which are in parentheses, the dispersion relation $E_{\mathbf{p}}=(\varepsilon_{\mathbf{p}}^2+\Delta_{\mathbf{p}}^2)^{1/2}$ and the gap $\Delta_{\mathbf{p}}$. The s and $d_{x^2-y^2}$-wave forms for the gap that we are considering are $\Delta_{\mathbf{p}}=\Delta_0(T)$ and $\Delta_{\mathbf{p}}=(\Delta_0(T)/2)(\cos p_x-\cos p_y)$, respectively. We also assume a BCS temperature dependence for the gap amplitude $\Delta_0(T)$, and choose $2\Delta_0(0)=4T_c$, for simplicity.[17]

First, the normal-state results on the spectral function are presented. Figure 1 shows $\mathrm{Im}\chi(\mathbf{q},\omega)$ versus $\mathbf{q}$ at different temperatures for $\omega=0.05t$. Here $\mathbf{q}$ moves along the dashed line shown schematically in the inset. As T is lowered from $0.30t$ to $0.10t$, the development of incommensurate antiferromagnetic fluctuations due to Fermi-surface nesting is clearly seen. For the band parameters and the filling that we are using, $\mathrm{Im}\chi(\mathbf{q},\omega)$ peaks at

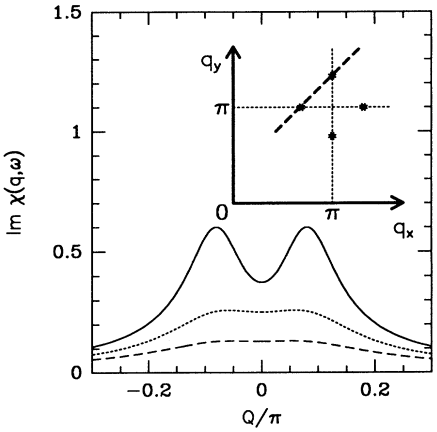

FIG. 1. Momentum dependence of $\mathrm{Im}\chi(\mathbf{q},\omega)$ in the normal state for temperatures $T=0.10t$ (solid line), $0.20t$ (dotted line), and $0.30t$ (dashed line). Here $\omega=0.05t$ and the momentum is scanned along $\mathbf{q}=(Q,Q)+[(1-\delta/2)\pi,(1+\delta/2)\pi]$ with $\delta=0.10$ as indicated by the dashed line in the inset.

$\mathbf{q}^*\simeq(0.9\pi,\pi)$. This shift depends upon details of the band structure and for a three-band Hubbard model with parameters adjusted to fit the La_2CuO_4 band structure, it can be a factor of 2 larger, in agreement[18,19] with experiments on $La_{2-x}Sr_xCuO_4$. Here for simplicity we will use the one-band near-neighbor form for ε_p discussed above.

As the incommensurate peak structure develops at $\mathbf{q}^*$, at $\mathbf{Q}=(\pi,\pi)$ we have from Eq. (2)

$$\mathrm{Im}\chi_0(\mathbf{Q},\omega)=\frac{\pi}{2}N\left[\frac{\omega}{2}\right]\left[f\left[|\mu|-\frac{\omega}{2}\right]-f\left[|\mu|+\frac{\omega}{2}\right]\right], \tag{4}$$

where $N(\omega)$ is the single-particle density of states given by $K[\sqrt{1-(\omega/4t)^2}]/2\pi^2t$ with K the elliptic integral of the first kind. From Eq. (4) we see that at low temperatures a kinematic gap[20,15] opens for $\omega\leq 2|\mu|$. This occurs in the normal state and simply reflects the fact that when the system is doped away from half-filling, the wave vectors near $\mathbf{Q}=(\pi,\pi)$ no longer span the Fermi surface. Hence at low temperatures, it takes a finite energy $2|\mu|$ to create a particle-hole pair with momentum $\mathbf{Q}=(\pi,\pi)$. Results for the normal-state RPA spectral weight $\mathrm{Im}\chi(\mathbf{q},\omega)$ versus T for two different frequencies at $\mathbf{q}=\mathbf{Q}$ and $\mathbf{q}=\mathbf{q}^*$ are shown in Fig. 2, where the occurrence of a kinematic gap for $\mathbf{q}=\mathbf{Q}$ is clearly evident.

Turning next to the superconducting case, we assume that a superconducting gap of s- or $d_{x^2-y^2}$-wave symmetry opens at $T_c=0.10t$. Results for $\mathrm{Im}\chi(\mathbf{q},\omega)$ versus $\mathbf{q}$ at $\omega=T_c/2$ obtained using s- and $d_{x^2-y^2}$-wave gap symmetries below T_c are shown in Figs. 3(a) and 3(b). For an s-wave gap there is a rapid suppression of the spectral weight for frequencies below 2Δ accompanied by a broadening of the peaks as T is lowered below T_c. As an s-wave gap opens, it acts like an effective temperature, suppressing $\chi_0(\mathbf{q},\omega)$. Thus at a reduced temperature $T/T_c=0.8$, where $2\Delta\simeq 0.3t$, the s-wave results for $\mathrm{Im}\chi(\mathbf{q},\omega)$ shown in Fig. 3(a) are similar to the normal-state behavior shown in Fig. 1 at a temperature $T=0.3t$.

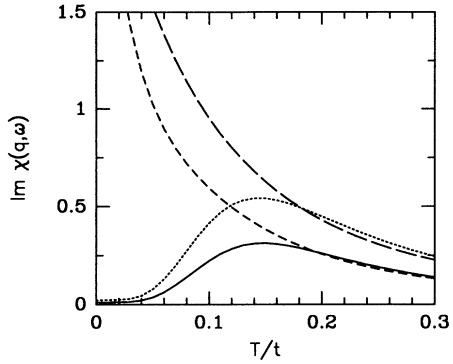

FIG. 2. $\mathrm{Im}\chi(\mathbf{q},\omega)$ vs T/t at $\mathbf{q}=\mathbf{q}^*=(0.9\pi,\pi)$ and $\mathbf{q}=\mathbf{Q}=(\pi,\pi)$ in the normal state. Here the solid and the dotted lines represent results for $\mathbf{q}=\mathbf{Q}$ at energy transfer $\omega=0.05t$ and $0.10t$, respectively. The dashed and the long-dashed lines are for $\mathbf{q}=\mathbf{q}^*$ at $\omega=0.05t$ and $0.10t$, respectively.

In the case of the $d_{x^2-y^2}$-wave gap symmetry, the results are quite different. As T is lowered from $T=T_c$ to $0.8T_c$, $\mathrm{Im}\chi(\mathbf{q},\omega)$ first decreases at all the $\mathbf{q}$ values shown due to the reduction in $\mathrm{Im}\chi_0(\mathbf{q},\omega)$ caused by the opening of the $d_{x^2-y^2}$-wave gap. However, because of the nodes, the real part of $\chi_0(\mathbf{q}^*,\omega)$ continues to gradually increase

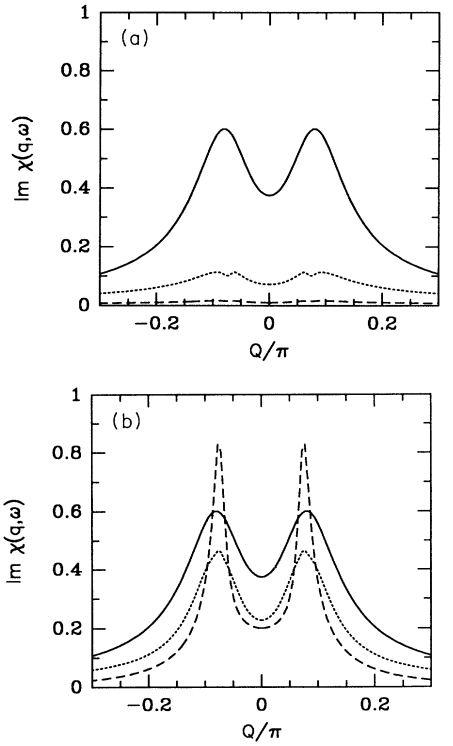

FIG. 3. Momentum dependence of $\mathrm{Im}\chi(\mathbf{q},\omega)$ in the superconducting state for (a) an s-wave gap and (b) a $d_{x^2-y^2}$-wave gap at $\omega=T_c/2$. For the s-wave gap, results are shown at $T=T_c$ (solid line), $0.8T_c$ (dotted line), and $0.5T_c$ (dashed line), whereas for the $d_{x^2-y^2}$-wave gap we use $T=T_c$ (solid line), $T=0.8T_c$ (dotted line), and $T=0.2T_c$ (dashed line). The momentum scan is the same as in Fig. 1.

as the temperature is lowered below T_c. This eventually leads to a narrowing of the peak structure as shown by the dashed curve in Fig. 3(b). That is,

$$\mathrm{Im}\chi(\mathbf{q},\omega)=\frac{\mathrm{Im}\chi_0(\mathbf{q},\omega)}{[1-U\,\mathrm{Re}\chi_0(\mathbf{q},\omega)]^2+[U\,\mathrm{Im}\chi_0(\mathbf{q},\omega)]^2}\ , \quad (5)$$

with χ_0 given by Eq. (3) for $T<T_c$. Thus when $\mathrm{Im}\chi_0(\mathbf{q}^*,\omega)$ decreases and $\mathrm{Re}\chi_0(\mathbf{q}^*,\omega)$ increases, as it can for the $d_{x^2-y^2}$-wave gap, the features near $\mathbf{q}^*$ can actually sharpen in the superconducting state.

The effects of the s- and $d_{x^2-y^2}$-wave gaps on $\mathrm{Im}\chi(\mathbf{q},\omega)$ are further contrasted in Figs. 4(a) and 4(b), where we have plotted $\mathrm{Im}\chi(\mathbf{q}^*,\omega)$ versus T/T_c at different ω values. An s-wave gap of $2\Delta_0(0)=4T_c$ suppresses[21] the spin fluctuations when $\omega<2\Delta$, while for a $d_{x^2-y^2}$-wave gap there is a competition between the decrease in $\mathrm{Im}\chi_0(\mathbf{q}^*,\omega)$ and the increase in $\mathrm{Re}\chi_0(\mathbf{q}^*,\omega)$ as we have discussed. For a $d_{x^2-y^2}$-wave gap, as the superconducting gap opens, $\mathrm{Im}\chi(\mathbf{q}^*,\omega)$ at low ω first decreases, and then starts to increase when $T\sim T_c/2$, eventually becoming larger than its value at T_c. The initial drop in $\mathrm{Im}\chi(\mathbf{q}^*,\omega)$ for low ω is due to the opening of the gap and the BCS coherence factors. For a $d_{x^2-y^2}$-wave gap with $\mathbf{q}^*$ near (π,π), we have $\Delta_{\mathbf{p}+\mathbf{q}^*}\simeq-\Delta_{\mathbf{p}}$ for a number of $\mathbf{p}$ points on the Fermi surface, hence the coherence factor of the first term in the expression for $\chi_0^{\mathrm{BCS}}(\mathbf{q},\omega)$ [Eq. (3)], corresponding to quasiparticle scattering, are reduced. This, along with the opening of a gap over much of the Fermi surface, causes $\mathrm{Im}\chi_0(\mathbf{q}^*,\omega)$ to decrease. The increase of $\mathrm{Im}\chi(\mathbf{q}^*,\omega)$ at lower T is due to the nodes of the $d_{x^2-y^2}$-wave gap, which as previously discussed, leads to a gradual increase in $\mathrm{Re}\chi_0(\mathbf{q}^*,\omega)$ at temperatures below T_c.

Experimentally, $\mathrm{Im}\chi(\mathbf{q},\omega)$ is convoluted by the resolution of the neutron-scattering apparatus, so that what is observed is an integral of $\mathrm{Im}\chi(\mathbf{q},\omega)$ over a region of $\mathbf{q}$ near $\mathbf{q}^*$. Typically, the resolution function is elongated in the direction perpendicular to the momentum scan. We have integrated the RPA $d_{x^2-y^2}$-wave results for $\mathrm{Im}\chi(\mathbf{q},\omega)$ over $\mathbf{q}$ perpendicular to the scanning path for a region $\Delta_{q\perp}=\pm0.1\pi/\sqrt{2}$, and the resulting integrated spectral weight is shown in Fig. 4(c). We also show in Fig. 4(d) results obtained by averaging over an area $\Delta_{q\perp}=\Delta_{q\parallel}=\pm0.1\pi/\sqrt{2}$ centered at $\mathbf{q}^*$, with $\Delta_{q\perp}$ and $\Delta_{q\parallel}$ being perpendicular and parallel respectively, to the dashed line shown in the inset of Fig. 1. From Figs. 4(b)–4(d) we see that the structure of the $d_{x^2-y^2}$ low-temperature spectral weight depends upon the $\mathbf{q}$ resolution of the measurement. Thus, limited instrumental resolution or sample quality can modify the characteristic $d_{x^2-y^2}$-wave behavior shown in Fig. 4(b). The dotted line in Fig. 4(b) is the s-wave result. For an s-wave gap, the integrated intensity vanishes for $\omega<2\Delta$ as $T\to0$.

In summary, we have explored the spin-fluctuation spectral weight using a simple model which takes into account both antiferromagnetic and superconducting correlations. Above the superconducting transition temperature, incommensurate spin fluctuations grow at momen-

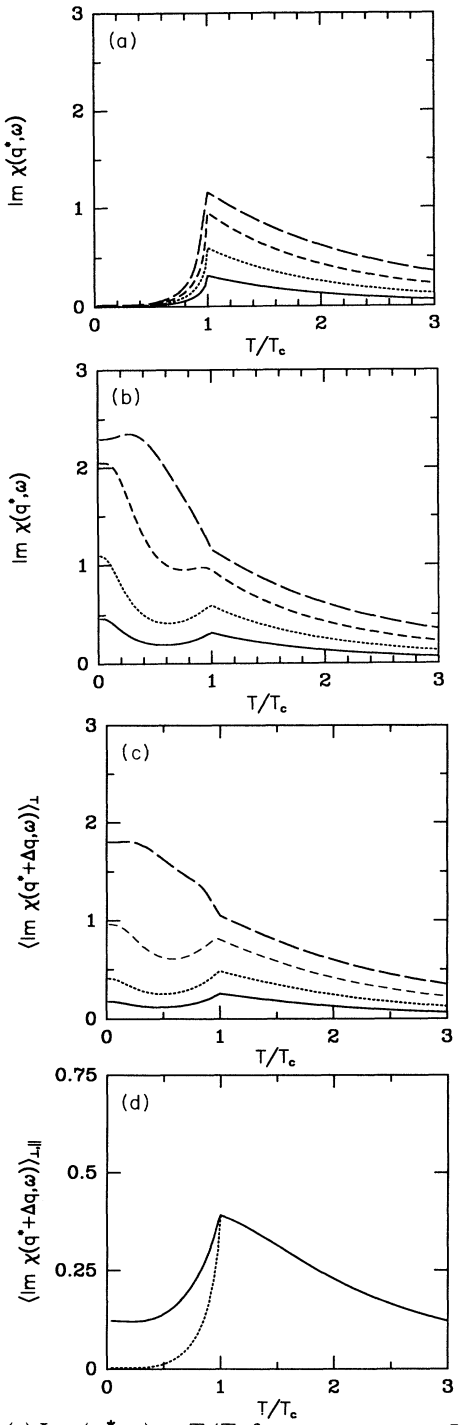

FIG. 4. (a) $\mathrm{Im}\chi(\mathbf{q}^*,\omega)$ vs T/T_c for an s-wave gap. Here the results are given at frequencies of $\omega=T_c/4$ (solid line), $T_c/2$ (dotted line), T_c (dashed line), and $2T_c$ (long-dashed line). (b) Same as (a) for a $d_{x^2-y^2}$-wave gap. (c) Integrated spectral weight $\langle\mathrm{Im}\chi(\mathbf{q}^*+\Delta\mathbf{q},\omega)\rangle_\perp$ vs T/T_c for a $d_{x^2-y^2}$-wave gap. Here the results are shown at the same frequencies as in (a) and the momentum average is done for $\Delta_{q\perp}=\pm0.1\pi/\sqrt{2}$. (d) Integrated spectral weight $\langle\mathrm{Im}\chi(\mathbf{q}^*+\Delta\mathbf{q},\omega)\rangle_{\perp,\parallel}$ vs T/T_c for $d_{x^2-y^2}$ (solid line) and s-wave (dotted line) gaps at $\omega=T_c/2$. Here the momentum average is done for $\Delta_{q\perp}=\pm0.1\pi/\sqrt{2}$ and $\Delta_{q\parallel}=\pm0.1\pi/\sqrt{2}$.

tum transfers shifted along the edges of the Brillouin zone while the low-frequency spectral weight near (π,π) is depressed by the opening of a kinematic gap. Below T_c, an s-wave gap leads to a rapid suppression of the incommensurate peak structure seen in a momentum scan. For a $d_{x^2-y^2}$-wave gap, the incommensurate peaks can continue to narrow and rise at low temperatures. For an s-wave gap,[22] the temperature dependence of the spectral weight for $\omega < 2\Delta$ observed near $\mathbf{q}^*$ is rapidly suppressed to zero as T drops below T_c. However, the spectral weight for a $d_{x^2-y^2}$-wave gap depends upon the $\mathbf{q}$ resolution and can remain significant for $T < T_c$.

The authors would like to thank G. Aeppli for extensive discussions regarding neutron scattering, for the physical insight he provided and his comments on the importance of averaging over the momentum resolution. One of the authors (N.B.) gratefully acknowledges financial support from IBM. This work was partially supported by the National Science Foundation under Grants DMR90-02492 and PHY89-04035, and the Electrical Power Research Institute. The numerical calculations reported in this paper were performed at the San Diego Supercomputer Center and the Supercomputer Computations Research Institute at the Florida State University.

[1]S-W. Cheong, G. Aeppli, T. E. Mason, H. Mook, S. M. Hayden, P. C. Canfield, Z. Fisk, K. N. Clausen, and J. L. Martinez, Phys. Rev. Lett. **67**, 1791 (1991).

[2]T. E. Mason, G. Aeppli, and H. A. Mook, Phys. Rev. Lett. **68**, 1414 (1992).

[3]J. M. Tranquada, P. M. Gehring, G. Shirane, S. Shamoto, and M. Sato (unpublished).

[4]B. J. Sternlieb, M. Sato, S. Shamoto, G. Shirane, and J. M. Tranquada (unpublished).

[5]T. R. Thurston, R. J. Birgeneau, Y. Endoh, P. M. Gehring, M. A. Kastner, H. Kojima, M. Matsuda, G. Shirane, I. Tanaka, and K. Yamada (unpublished).

[6]J. Rossat-Mignod, L. P. Regnault, C. Vettier, P. Bourges, P. Burlet, J. Bossy, J. Y. Henry, and G. Lapertot, Physica (Amsterdam) **185-189**, 86 (1991).

[7]N. Bulut, D. Hone, D. J. Scalapino, and N. E. Bickers, Phys. Rev. B **41**, 1797 (1990); Phys. Rev. Lett. **64**, 2723 (1990).

[8]N. Bulut and D. J. Scalapino, Phys. Rev. B **45**, 2371 (1992); Phys. Rev. Lett. **68**, 706 (1992).

[9]N. Bulut and D. J. Scalapino, Phys. Rev. Lett. **67**, 2898 (1991).

[10]N. Bulut, in *Dynamics of Magnetic Fluctuations in High Temperature Superconductors,* edited by G. Reiter, P. Horsch, and G. Psaltakis (Plenum, New York, 1991).

[11]L. Chen, C. Bourbonnais, T. Li, and A.-M. S. Tremblay, Phys. Rev. Lett. **66**, 369 (1991).

[12]N. Bulut, D. J. Scalapino, and S. R. White (unpublished).

[13]R. Joynt and T. M. Rice, Phys. Rev. B **38**, 2345 (1988), have discussed the problem of identifying the symmetry of the superconducting gap using neutron scattering.

[14]J. P. Lu, Phys. Rev. Lett. **68**, 125 (1992), has reported results for $\mathrm{Im}\chi_0(\mathbf{q},\omega)$ for an s- and a d-wave gap. For a d-wave gap, he finds that the peaks in the scattering intensity occur along the diagonal $q_x = q_y$ rather than the edges of the zone $(\pi\pm\delta,\pi)$ as we do. This is because he has chosen a chemical potential $\mu/t = -1.0$, which gives a filling $\langle n \rangle \sim 0.6$ sufficiently far from half-filling. In addition, he does not take into account the enhancement of the spin fluctuations due to U.

[15]N. Bulut and D. J. Scalapino (unpublished).

[16]In this paper we have chosen $U = 2t$ and $\langle n \rangle = 0.85$ for simplicity. Qualitative features of the results presented here do not vary with small changes in U and $\langle n \rangle$.

[17]A discussion of the BCS spectral weight $\mathrm{Im}\chi_0^{\mathrm{BCS}}(\mathbf{q},\omega)$ was given by D. J. Scalapino, in *High Temperature Superconductivity,* edited by K. S. Bedell, D. Coffey, D. Meltzer, D. Pines, and J. R. Schrieffer (Addison-Wesley, Reading, 1990).

[18]P. B. Littlewood, J. Zaanen, G. Aeppli, and H. Monien (unpublished).

[19]Q. Si, Y. Zha, K. Levin, J. P. Lu, and J. H. Kim (unpublished).

[20]S. Wermbter and L. Tewordt, Phys. Rev. B **43**, 10 530 (1991).

[21]S. Wermbter and L. Tewordt, Phys. Rev. B **44**, 9524 (1991), have studied a model with an s-wave gap in which they find that $\mathrm{Im}\chi(\mathbf{q},\omega)$ exhibits a pseudo gap with a gradual decrease of the spectral weight for $\omega < 2\Delta$ as T decreases. In this work, the additional spectral weight below 2Δ arises from pair-breaking lifetime effects.

[22]An analysis of the response for a gapless s-wave state is in progress, G. Aeppli, N. Bulut, and D. J. Scalapino (unpublished).